Age-related brainstem degeneration through microRNA modulation in mice

RIE KAWAKITA[1*], TADAYUKI TAKATA[1*], WAKAKO NONAKA[1,2], YASUHIRO HAMADA[1], HISAKAZU IWAMA[3], HIDEKI KOBARA[4], KAZUSHI DEGUCHI[1], OSAMU MIYAMOTO[5], TAKEHIRO NAKAMURA[6], TOSHIFUMI ITANO[1] and TSUTOMU MASAKI[4]

Departments of [1]Neurology and [2]General Medicine; [3]Life Science Research Center; [4]Department of Gastroenterology, Faculty of Medicine, Kagawa University, Miki, Kagawa 761-0793; [5]Department of Medical Engineering, Faculty of Health Science and Technology, Kawasaki University of Medical Welfare, Kurashiki, Okayama 701-0193; [6]Department of Physiology 2, Kawasaki Medical School, Kurashiki, Okayama 701-0192, Japan

Received December 20, 2022; Accepted May 12, 2023

DOI: 10.3892/mmr.2023.13032

Abstract. Histopathological changes occur in the brainstem during the early stages of Alzheimer's disease (AD), with the pathological changes of the brain lesions ascending progressively in accordance with the Braak staging system. The senescence-accelerated mouse prone 8 (SAMP8) mouse model has been previously used as a model of age-dependent neurodegenerative diseases, including AD. In the present study, microRNAs (miRNAs) that were upregulated or downregulated in SAMP8 brainstems were identified using miRNA profiling of samples obtained from miRNA arrays. The preliminary stage of cognitive dysfunction was examined using male 5-month-old SAMP8 mice, with age-matched senescence-accelerated mouse resistant 1 mice as controls. A Y-maze alternation test was performed to assess short-term working memory and miRNA profiling was performed in each region of the dissected brain (brainstem, hippocampus and cerebral cortex). SAMP8 mice tended to be hyperactive, but short-term working memory was preserved. Two miRNAs were upregulated (miR-491-5p and miR-764-5p) and two were downregulated (miR-30e-3p and miR-323-3p) in SAMP8 brainstems. In SAMP8 mice, the expression level of upregulated miRNAs were the highest in the brainstem, wherein age-related brain degeneration occurs early. It was demonstrated that the order of specific miRNA expression levels corresponded to the progression order of age-related brain degeneration. Differentially expressed miRNAs regulate multiple processes, including neuronal cell death and neuron formation. Changes in miRNA expression may result in the induction of target proteins during the early stages of neurodegeneration in the brainstem. These findings suggest that studying altered miRNA expression may provide molecular evidence for early age-related neuropathological changes.

Correspondence to: Dr Tadayuki Takata, Department of Neurology, Faculty of Medicine, Kagawa University, 1750-1 Ikenobe, Miki, Kita, Kagawa 761-0793, Japan
E-mail: tadayukitakata1115@gmail.com

*Contributed equally

Abbreviations: miRNA, microRNA; AD, Alzheimer's disease; PD, Parkinson's disease; SAMP8, senescence-accelerated mouse prone 8; SAMR1, senescence-accelerated mouse resistant 1; H&E, hematoxylin and eosin; SSC, saline-sodium citrate; FC, fold change; GFAP, glial fibrillary acidic protein; RT-qPCR, reverse transcription-quantitative polymerase chain reaction; mmu, *Mus musculus*; APP, amyloid precursor protein; PTEN, phosphatase and tensin homolog; TGF, transforming growth factor; NG2, neuronal-glial antigen 2; NINJ2, ninjurin 2

Key words: microRNA, brainstem, neurodegeneration, SAMP8 mouse, aging

Introduction

MicroRNAs (miRNAs) are small, single-stranded RNAs that do not encode proteins. MiRNAs repress the translation of target mRNAs to regulate gene expression (1) and serve an important role in the mechanism of age-related changes in the brain (2,3). In our previous study, it was suggested that certain miRNAs may play important roles in neurodegenerative diseases, such as inducing the accumulation of α-synuclein (4) and targeting molecules related to the autophagy pathway (5).

Aging is one of the major risk factors for neurodegenerative diseases, including Alzheimer's disease (AD) and Parkinson's disease (PD) (6). Pathological changes in the brain associated with AD have been demonstrated to first occur in the locus coeruleus of the brainstem before the onset of the disease (7) followed by spread to the hippocampus and involvement of the cerebral cortex in the terminal stages of the disease (8). Furthermore, early pathological changes in the dorsal motor nucleus of the glossopharyngeal and vagal nerves of the brainstem occur and progress to the hippocampus and cerebral cortex in an ascending manner in sporadic PD (9). The brainstem exhibits pathological changes from an early stage

in certain neurodegenerative diseases such as AD (7,8) and PD (9); however, the molecular mechanisms encompassing these changes remain unknown.

Senescence-accelerated mouse prone 8 (SAMP8) mice are used as animal models of rapid aging and show age-related deficits in learning and memory (10,11). Thus, SAMP8 mice may be a useful model for studying neurodegenerative changes associated with AD (10). There have been numerous reports on the histopathological brain degeneration of SAMP8 mice at each week age and the order of the progression (11-13). SAMP8 mice show spongiform degeneration in the brainstem at 1 month of age, with maximum spongiosis observed at 4-8 months (14). These histopathological changes suggest that age-related brain degeneration progresses from the brainstem in SAMP8 mice, which is similar to that in humans (7-9). By contrast, senescence-accelerated mouse resistant 1 (SAMR1) mice demonstrate behaviorally normal senescence patterns (10). Furthermore, SAMR1 mice exhibit no spongiform degeneration in any brain region in early postnatal age (12). As a result of these characteristics, SAMR1 mice are frequently used as controls for SAMP8 mice. The present study aimed to assess the early-stage pathological degeneration in the brainstem of SAMP8 mice and identify specific miRNAs involved in early-stage brain pathological degeneration in the brainstem through miRNA profiling of each brain region in SAMP8 and SAMR1 mice.

Materials and methods

Animals. Twelve 5-month-old male SAMR1 and SAMP8 mice (n=6/strain; Japan SLC, Inc.) weighing 30-40 g were used in this study. The present study was approved by the Animal Committee of the Kagawa University School of Medicine (approval number: 20626-2). The mice were housed under controlled environmental conditions, including a temperature range of 22-24˚C, 40-60% humidity and 12 h light-dark cycles. All mice had *ad libitum* access to water and food and received two daily health observations. The study employed humane endpoints, including labored breathing, nasal discharge, lethargy or persistent recumbency, difficulty with ambulation or an inability to obtain food or water. The experiment duration was limited to the acclimation period of the animals to the facility. After neurobehavioral evaluation, all 12 mice were sacrificed using intraperitoneal pentobarbital (150 mg/kg). After confirming the absence of breathing, perfusion with physiological saline solution was initiated. Euthanasia was confirmed by the absence of cardiac activity during perfusion, following which perfusion fixation was performed using paraformaldehyde. Following euthanasia, the brains of the mice were removed to be used in subsequent analyses. After perfusion fixation, the samples for miRNA profiling were placed in RNAlater (cat. no. AMB AM7024; Thermo Fisher Scientific, Inc.) and stored at -80˚C, while those for histological evaluation were placed in 4% paraformaldehyde and stored in a refrigerator at 4˚C. The brains were divided into the hippocampus, brainstem and cerebral cortex, and the miRNA expression profiles were evaluated in these three regions. miRNA profiling was performed using five mice from each strain. Histological evaluation was performed on the single remaining mouse from each strain.

Behavioral test. The Y-maze alternation test was performed to assess short-term working memory in mice. The mice were allowed to enter the maze for 8 min and the maze arms into which they entered were recorded. The number of times a mouse entered each maze arm within the measured time (total number of arms entered) and the number of combinations that included three different arms entered in succession (number of alternations) were recorded. The alternation behavior rate (%) was calculated as follows: Alternation behavior rate %=number of alternations/(total number of arms entered-2) x100.

Histopathological analyses. Histopathological analyses were performed to confirm that histopathological changes in the SAMP8 mouse brains had occurred, as previously reported (11-13). Hematoxylin and eosin (H&E) staining and glial fibrillary acidic protein (GFAP) immunostaining were performed following paraffin-embedded tissue sectioning (6 μm thick) of the coronal plane. Paraffin (Merck & Co., Inc.) was utilized for tissue embedding and two cycles of infiltration at 64˚C were carried out for 30 min, followed by two cycles of infiltration at 64˚C for 1 h. In H&E staining, the hematoxylin staining was conducted for a duration of 3 min, followed by a 5-min water rinse at 40˚C. Subsequently, eosin staining was performed for 4 min. Following H&E staining, the brain regions of SAMP8 and SAMR1 mice were imaged using a light microscope to confirm spongiform degeneration in the brainstems of SAMP8 mice. The primary antibodies used were rabbit monoclonal antibodies against GFAP (1:400; cat. no. TA301159; Cosmo Bio Co., Ltd.). Anti-rabbit IgG goat polyclonal antibody, included in the Leica® BOND Polymer Refine Detection kit (cat. no. DS9800; Leica Biosystems, Inc.) was used as the secondary antibody. Selected sections were immunostained using the BOND III system (Leica Biosystems, Inc.) according to the manufacturer's instructions. The reaction of the primary antibody was conducted at room temperature for 15 min. The secondary antibody reaction was performed at room temperature for 8 min. The staining was visualized with 3,3'-diaminobenzidine. Anti-GFAP antibody-positive astrocytes were assessed in each of the stained sections.

RNA isolation. The total RNA was extracted from the tissue samples using the miRNeasy Mini Kit (Qiagen, Inc.) according to the manufacturer's instructions. RNA integrity was determined using a NanoDrop™ 2000 spectrophotometer (Thermo Fisher Scientific, Inc.). Total RNA quality was determined using RNA Nano 6000 chips from an Agilent 2100 Bioanalyzer (Agilent Technologies, Inc.) according to the manufacturer's protocol. Briefly, total RNA from all brain samples was heated at 70˚C for 2 min and incubated on ice for 5 min. Subsequently, the samples (1 μl) were loaded into each lane of the RNA Nano 6000 chips and the bands of 18S and 28S ribosomal RNA in the gel (RNA6000 Nano Gel Matrix; cat. no. 5067-1511; Agilent Technologies, Inc.) were detected using the Agilent 2100 Bioanalyzer. The RNA samples were stored at -80˚C.

miRNA arrays. The total RNA was labeled with Hy3 dye using the miRCURY LNA microRNA Array Hi-Power labeling kit (Exiqon A/S; Qiagen, Inc.). Total RNA (2 μg) was incubated with a spike protein (spike control for enzymatic labeling; cat. no. TRT-X304; Toray Industries, Inc.) for 30 min at 37˚C

and then at 95˚C for 5 min. Hy3 dye and Hi-Power labeling enzymes were added to each sample. The enzyme was heat inactivated at 16˚C for 1 h and 65˚C for 15 min and protected from light. The samples were loaded onto the arrays by capillary force using 3D-Gene miRNA oligo chips (version 21; cat. no. CM501; Toray Industries, Inc.). The chips enabled the examination of the expression of 679 miRNAs printed in duplicate spots. The arrays were incubated at 32˚C for 16 h, briefly washed at 30˚C with washing buffer solution [0.5X saline-sodium citrate (SSC), 0.1% sodium dodecyl sulfate (SDS)], rinsed with washing buffer solution (0.2X SSC, 0.1% SDS) and washed again in another buffer solution (0.05X SSC), according to the manufacturer's instructions (Toray Industries, Inc.). The arrays were centrifuged at 600 x g for 1 min at room temperature, followed by immediate scanning using a 3D-Gene 3000 miRNA microarray scanner (Toray Industries, Inc.). The relative miRNA expression levels were calculated by comparing the average signal intensities of the valid spots with their mean values throughout the microarray experiments, following normalization to their adjusted median values. The microarray data obtained in this study have been deposited in NCBI's Gene Expression Omnibus (GEO) database with accession number GSE228946 (https://www.ncbi.nlm.nih.gov/geo/query/acc.cgi?acc=GSE228946).

Quantification of miRNA. RNA isolation was performed using the miRNeasy Mini Kit (Qiagen, Inc.) and spiked with control sno-RNA-202 (Qiagen, Inc.), according to the manufacturer's protocol (Assay ID: 001232 for sno-RNA-202). Complementary DNA was synthesized for each target miRNA using the miRNA Reverse Transcription Kit (Thermo Fisher Scientific, Inc.), according to the manufacturer's protocol. miRNA expression was detected using reverse transcription-quantitative polymerase chain reaction (RT-qPCR) with TaqMan miRNA Assay and TaqMan Universal Master Mix II (Thermo Fisher Scientific, Inc.), according to the manufacturer's protocol (Assay IDs: 001630 for miR-491-5p; 002031 for miR-764-5p; 000422 for miR-30e-3p; 002227 for miR-323-3p). Thermocycling conditions were as follows: initial denaturation at 95˚C for 10 min, followed by 40 cycles at 95˚C for 15 sec and 60˚C for 60 sec. The relative miRNA expression levels were calculated using the comparative $2^{-\Delta\Delta Cq}$ method (15) and normalized to sno-RNA-202 expression. Experiments were performed in triplicate.

miRNA target gene bioinformatics analysis. The target genes of the identified miRNAs were predicted using the miRDB (https://mirdb.org), Targetscan 8.0 (https://www.targetscan.org/mmu_80/) and miRTarBase version 9.0 (https://mirtarbase.cuhk.edu.cn/~miRTarBase/miRTarBase_2022/php/index.php) databases. To enhance the reliability of the bioinformatics analysis, overlapping genes in two or three databases were identified during the analysis. To explore the relationships among target genes of identified miRNAs, we employed a Sankey diagram generated using Power-user software v1.6.1575 (https://www.powerusersoftwares.com).

Statistical analysis. Statistical analyses were performed using SPSS software (version 26.0; IBM Corp.). P<0.05 was considered to indicate a statistically significant difference. Alternation behavior rate, locomotor activity counts, signal intensities and ΔCq value are expressed as mean ± SD. Significant differences in the alternation behavior rate and locomotor activity data were assessed using an unpaired Student's t-test. The signal intensities of the miRNA probes were $\log_2$ transformed and quantile normalized, and then an unpaired Student's t-test was performed. Fold change (FC) was calculated from the non-$\log_2$ transformed signal intensities. miRNAs were considered differentially expressed if P<0.05 and FC>1.5 or FC<1.5^{-1}. Two-way ANOVA was performed with PORTION (mice: SAMP8 or SAMR1) and STATE (brain region: brainstem, hippocampus, and cerebral cortex) as factors for miRNA signal intensities and ΔCq value in each brain region of SAMP8 and SAMR1. Significances of individual differences were evaluated using Tukey's post-hoc test if ANOVA results were significant.

Selection processes of SAMP8 brainstem specifically regulated miRNAs. The three brain regions of interest, the cerebral cortex, hippocampus and brainstem, are denoted as C, H and B, respectively, and SAMP8 and SAMR1 mice are denoted as P or R, respectively. A set of differentially expressed miRNAs was represented as $\{\boldsymbol{d}_{(\mathbf{B|P>H|P})}\}$, where the expression of each miRNA of SAMP8 (P) in the brainstem (B) was significantly higher than that of SAMP8 (P) in the hippocampus (H). The set (α) of miRNAs whose expression was the highest in the brainstems of mice P among the three regions was defined as:

$$\boldsymbol{\alpha} = \{\boldsymbol{d}_{(\mathbf{B|P>H|P})}\} \cap \{\boldsymbol{d}_{(\mathbf{B|P>C|P})}\} \quad (1).$$

Similarly, the set (β) of miRNAs whose expression was the highest in the brainstem of mice R among the three regions was defined as:

$$\boldsymbol{\beta} = \{\boldsymbol{d}_{(\mathbf{B|R>H|R})}\} \cap \{\boldsymbol{d}_{(\mathbf{B|R>C|R})}\} \quad (2).$$

The set (γ) of miRNAs whose expression was the highest exclusively in mice P but not in mice R was defined as:

$$\boldsymbol{\gamma} = \boldsymbol{\alpha} \cap \neg\boldsymbol{\beta} \quad (3).$$

However, the members of γ did not guarantee that the expression of every miRNA was higher in the brainstems of mice P than in that of mice R. Therefore, from set γ, the miRNAs whose expression was significantly higher in mice P than in mice R were selected. These miRNAs were regarded as the SAMP8 brainstem specifically upregulated miRNAs, which were denoted as set δ and defined as:

$$\boldsymbol{\delta} = \boldsymbol{\gamma} \cap \{\boldsymbol{d}_{(\mathbf{B|P>B|R})}\} \quad (4).$$

A set (δ') of SAMP8 brainstem specifically downregulated miRNAs were obtained in a similar manner, using the following equations:

$$\boldsymbol{\alpha}' = \{\boldsymbol{d}_{(\mathbf{B|P<H|P})}\} \cap \{\boldsymbol{d}_{(\mathbf{B|P<C|P})}\} \quad (5),$$

$$\boldsymbol{\beta}' = \{\boldsymbol{d}_{(\mathbf{B|R<H|R})}\} \cap \{\boldsymbol{d}_{(\mathbf{B|R<C|R})}\} \quad (6),$$

$$\boldsymbol{\gamma}' = \boldsymbol{\alpha}' \cap \neg\boldsymbol{\beta}' \quad (7),$$

$$\boldsymbol{\delta}' = \boldsymbol{\gamma}' \cap \{\boldsymbol{d}_{(\mathbf{B|P<B|R})}\} \quad (8).$$

These equations were utilized to ensure the reproducibility of the data analysis regarding the selection processes

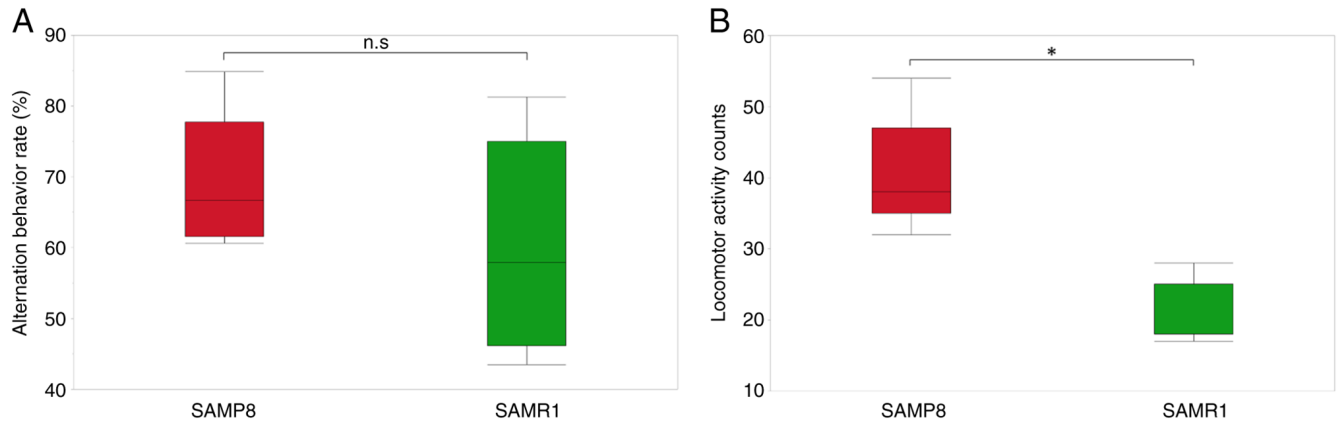

Figure 1. SAMP8 and SAMR1 mouse behavior assessed using (A) the alternation behavior rate and (B) locomotor activity counts using a Y maze test. (A) F 1, 12=1.076, (B) F 1, 12=34.5. Data are presented from n=6 mice/strain. The results are shown as mean ± SD. *P<0.05. n.s., not significant; SAMP8, senescence-accelerated mouse prone 8; SAMR1, senescence-accelerated mouse resistant 1.

of differentially expressed miRNAs. The equations were established in the present study and are presented without referencing any currently published papers, books or established software.

Results

Behavioral deficits in SAMP8 mice. Behavioral deficits were assessed in SAMP8 mice by comparing their behaviors with those of SAMR1 mice in the Y-maze. There was no significant difference in the alternation behavior rate between SAMP8 and SAMR1 mice (Fig. 1A). Locomotor activity counts were significantly higher in SAMP8 mice compared with those in SAMR1 mice (Fig. 1B). These results suggested that hyperactivity may occur as a behavioral change in the early postnatal period when cognitive deficits have not yet occurred.

Histopathological analysis of SAMP8 brain. Histological evaluation of the brains of SAMP8 and SAMR1 mice was performed to confirm that the pathological changes in 5-month-old SAMP8 mice were consistent with previously reports (8-10). Spongiform degeneration was observed in the reticular formation of the brainstem in the SAMP8 mouse (Fig. 2B-a) but not in an age-matched SAMR1 mouse (Fig. 2A-a). Vacuoles were also observed in the reticular formation of the SAMP8 brainstem (Fig. 2B-a) but not in the hippocampus or cortex of the SAMP8 mouse (Fig. 2B-b and c) or any brain region of the SAMR1 mouse tested (Fig. 2A). An increase in anti-GFAP antibody-positive astrocyte numbers was observed in the SAMP8 brainstem (Fig. 3B-a) compared with the SAMR1 brainstem (Fig. 3A-a). However, no noticeable increase in anti-GFAP antibody-positive astrocyte numbers was demonstrated in the hippocampus or cortex of the SAMP8 mouse (Fig. 3B-b, c) or any of the brain regions of the SAMR1 mouse (Fig. 3A).

Identification of differentially expressed miRNAs in SAMP8 and SAMR1 brainstems. The miRNA signal intensities were compared across each brain region (brainstem, hippocampus and cerebral cortex) and miRNAs that were upregulated or downregulated in the brainstems of SAMP8 mice were identified. Compared with those in the hippocampus and cerebral cortex, 72 and 34 miRNAs were upregulated in the brainstem, respectively. Using Equation 1, 18 miRNAs were identified with a significantly increased expression in the brainstem compared with the hippocampus and cerebral cortex of SAMP8 mice (Fig. 4A). In SAMP8 mice, 100 and 56 miRNAs were downregulated in the brainstem compared with those in the hippocampus and cerebral cortex, respectively. Additionally, 40 miRNAs were identified with significantly decreased expression in the brainstem compared with the hippocampus and cerebral cortex in SAMP8 mice (Fig. 4B, Equation 5).

Similarly, the miRNA signal intensities were compared across each brain region in SAMR1 mice. Compared with those in the hippocampus, 27 upregulated and 47 downregulated miRNAs were identified in the brainstem and 41 upregulated and 49 downregulated miRNAs were identified in the brainstem compared with those in the cortex. Using Equation 2, 18 miRNAs were demonstrated to have a significantly higher expression in the brainstem than in the hippocampus and cerebral cortex in SAMR1 mice (Fig. 4A). Finally, 28 miRNAs with a significantly lower expression in the brainstem than in the hippocampus and cerebral cortex in SAMR1 mice were identified (Fig. 4B, Equation 6).

Identification of SAMP8-brainstem-specifically regulated miRNAs. Examination of the miRNAs with the highest and lowest expression in the brainstems of SAMP8 mice was performed. Using Equation 3, five miRNAs were identified with the highest expression exclusively found in the SAMP8 brainstem. These were *Mus musculus* (mmu)-miR-204-5p, mmu-miR-3552, mmu-miR-491-5p, mmu-miR-6968-5p and mmu-miR-764-5p (Fig. 4A). Similarly, 14 miRNAs with the lowest expression in the brainstem exclusively found in SAMP8 mice were identified. These were mmu-miR-101a-3p, mmu-miR-101c, mmu-miR-212-3p, mmu-miR-212-5p, mmu-miR-218-5p, mmu-miR-30e-3p, mmu-miR-323-3p, mmu-miR-337-3p, mmu-miR-376b-5p, mmu-miR-3962, mmu-miR-674-3p, mmu-miR-708-3p, mmu-miR-708-5p and mmu-miR-7a-1-3p (Fig. 4B, Equation 7). It was then assessed whether the expression intensity of each of the five

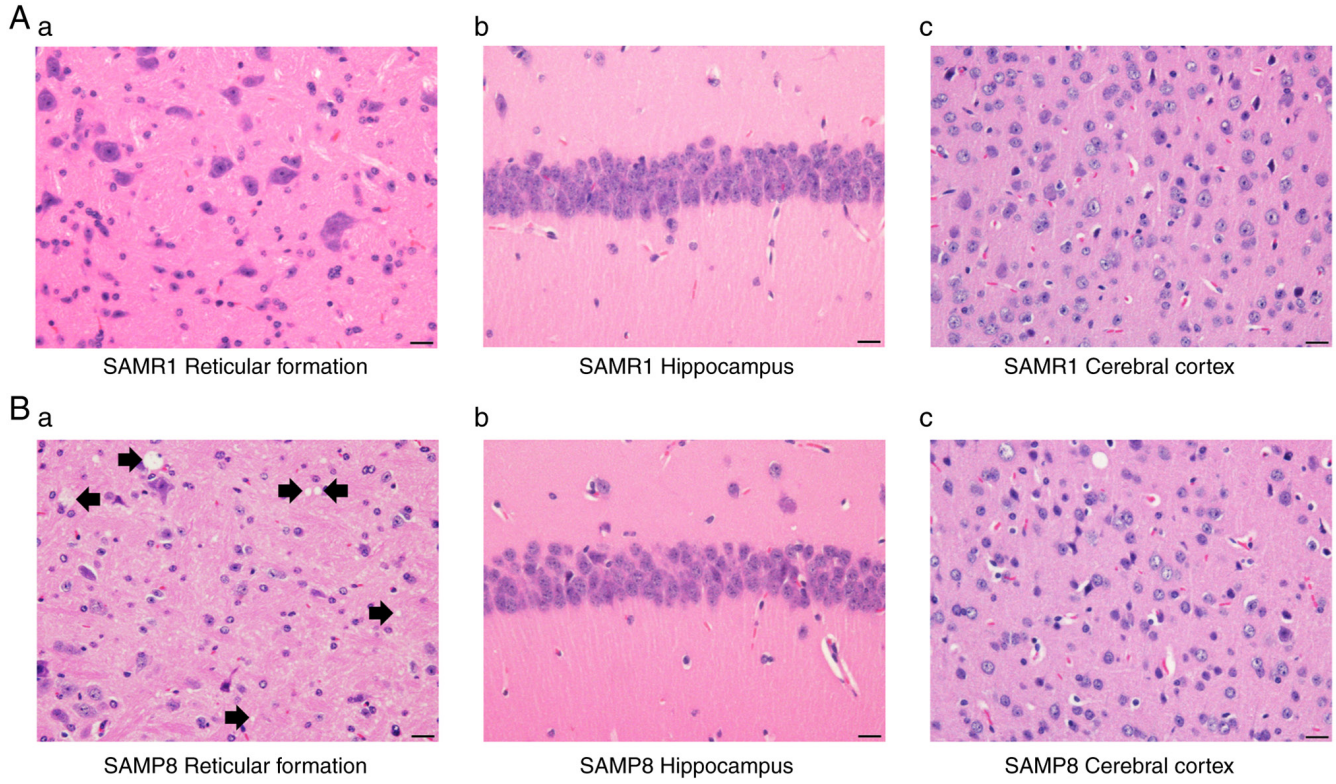

Figure 2. Hematoxylin and eosin staining in (A) SAMR1 and (B) SAMP8 mice in the (a) reticular formation of brainstem, (b) hippocampus and (c) cerebral cortex at high magnification. Black arrows indicate the presence of vacuoles. Scale bar, 20 μm. SAMR1, senescence-accelerated mouse resistant 1; SAMP8, senescence-accelerated mouse prone 8.

miRNAs with the highest expression in SAMP8 brainstems (mmu-miR-204-5p, mmu-miR-3552, mmu-miR-491-5p, mmu-miR-6968-5p and mmu-miR-764-5p) was higher when compared with SAMR1 brainstems. The miRNA signal intensities in the brainstems of SAMR1 and SAMP8 mice were compared and a set of 85 miRNAs were obtained that were significantly upregulated in SAMP8 mice. Thereafter, using Equation 4, two miRNAs were identified that may be considered as SAMP8 brainstem specifically upregulated miRNAs: Mmu-miR-491-5p and mmu-764-5p (Fig. 5A, Table I). Correspondingly, 86 miRNAs were found to be significantly downregulated in the brainstem of SAMP8 mice compared with those in SAMR1 mice. Two SAMP8 brainstem specifically downregulated miRNAs were identified: Mmu-30e-3p and mmu-miR-323-3p (Fig. 5B, Table I, Equation 8). Fig. 6 presents the upregulated miRNAs, miR-491-5p and miR-764-5p (spots 1 and 2, respectively), and the downregulated miRNAs, miR-30e-3p and miR-323-3p (spots 3 and 4, respectively), in the SAMP8 mouse brainstem analyzed using a miRNA chip.

Quantification of the expression levels of mmu-miR-491-5p and mmu-miR-764-5p. In SAMP8 mice, the mmu-miR-491-5p signal intensity was significantly higher in the brainstem (6.49±0.42) compared with that in the hippocampus (5.69±0.38) (P=0.040) or cerebral cortex (5.66±0.34) (P=0.031) (Fig. 7A, Table II). Similarly, the mmu-miR-764-5p signal intensity was significantly higher in the brainstem (4.81±0.49) compared with that in the hippocampus (4.04±0.25) (P=0.013) or cerebral cortex (4.13±0.36) (P=0.036) of SAMP8 mice (Fig. 7B, Table II). However, there was no significant difference in the signal intensities of mmu-miR-764-5p in the brainstem (3.82±0.30) compared with that in the hippocampus (3.63±0.32) (P=0.932) or cortex (3.56±0.16) (P=0.805) of SAMR1 mice (Fig. 7B, Table II). Additionally, there was no significant difference in signal intensities of mmu-miR-491-5p in SAMR1 mice in the brainstem (5.72±0.56) compared with that in the cortex (4.97±0.31) (P=0.058) and the hippocampus (5.18±0.31) (P=0.279) (Fig. 7A, Table II).

The expression of mmu-miR-491-5p and mmu-miR-764-5p was determined using RT-qPCR to validate the miRNA array data (Table III). In SAMP8 mice, the mean ΔCq ± standard deviation for mmu-miR-491-5p was 1.64±1.35 in the brainstem, 1.15±0.60 in the hippocampus and 1.53±1.45 in the cerebral cortex, while the mean ΔCq ± standard deviation for mmu-miR-764-5p was 2.10±2.23 in the brainstem, 1.32±0.96 in the hippocampus and 10.51±21.98 in the cerebral cortex (Fig. 8A and B, Table III). In SAMR1 mice, the values for mmu-miR-491-5p were 1.15±0.81, 1.05±0.39 and 1.48±1.80 (Fig. 8A, Table III) and those for mmu-miR-764-5p were 1.42±1.49, 1.19±0.83 and 2.17±3.49 in the brainstem, hippocampus and cerebral cortex, respectively (Fig. 8B, Table III). Overall, there were no significant differences in the miRNA expression levels, determined using RT-qPCR, between brain regions of SAMP8 and SAMR1 mice.

Quantifications of mmu-miR-30e-3p and mmu-miR-323-3p. In SAMP8 mice, the mmu-miR-30e-3p signal intensity was significantly lower in the brainstem (5.74±0.45) compared with the hippocampus (6.53±0.28) (P=0.015); however, there was no

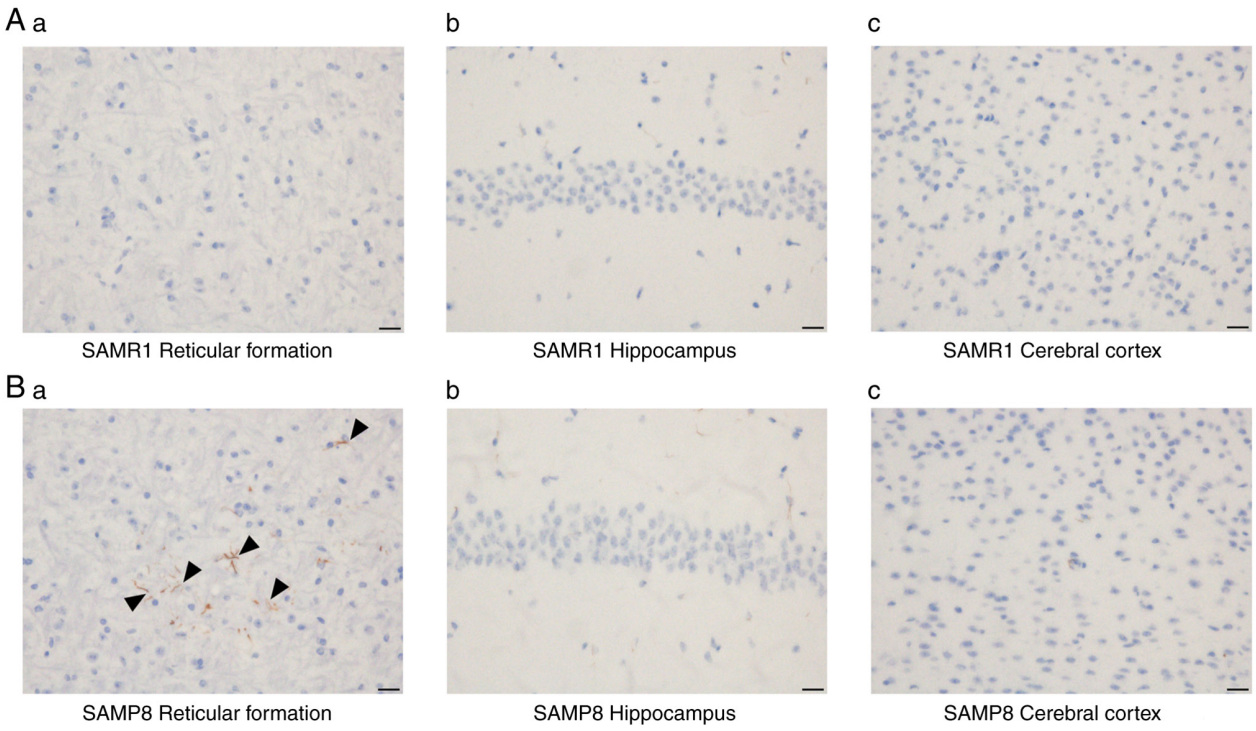

Figure 3. Glial fibrillary acidic protein immunostaining in (A) SAMR1 and (B) SAMP8 mice in the (a) reticular formation of brainstem, (b) hippocampus and (c) cerebral cortex at high magnification. Black arrowheads indicate the presence of anti-GFAP antibody-positive astrocytes. Scale bar, 20 μm. SAMR1, senescence-accelerated mouse resistant 1; SAMP8, senescence-accelerated mouse prone 8.

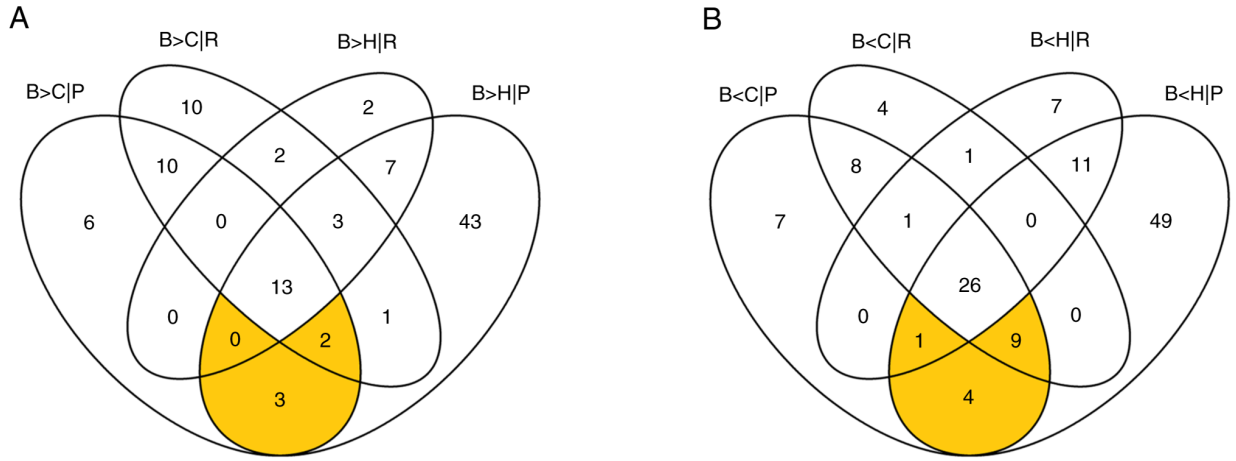

Figure 4. Venn diagrams of differentially expressed miRNAs in the brainstem compared with those in the hippocampus and cerebral cortex of SAMP8 and SAMR1 mice. (A) miRNAs with the highest expression. B>H|P and B>C|P indicate the upregulated miRNAs in the brainstem compared with those in the hippocampus and cerebral cortex, respectively, of SAMP8 mice. B>H|R and B>C|R indicate the upregulated miRNAs in the brainstem compared with the hippocampus and cerebral cortex, respectively, in SAMR1 mice. (B) miRNAs with the lowest expression. B<H|P and B<C|P indicate the downregulated miRNAs in the brainstem compared with those in the hippocampus and cerebral cortex, respectively, in SAMP8 mice. B<H|R and B<C|R indicate the downregulated miRNAs in the brainstem compared with those in the hippocampus and cerebral cortex, respectively, in SAMR1 mice. SAMP8 (P), senescence-accelerated mouse prone 8; SAMR1 (R), senescence-accelerated mouse resistant 1; B, brainstem; H, hippocampus; C, cerebral cortex; miRNA, micro RNA.

significant difference in the signal intensities of mmu-miR-30e-3p in SAMP8 mice between the brainstem and the cerebral cortex (6.35±0.39) (P=0.866) (Fig. 7C, Table II). Similarly, the mmu-miR-323-3p signal intensity in SAMP8 mice was significantly lower in the brainstem (2.44±0.92) compared with that in the hippocampus (4.01±0.41) (P=0.014). Additionally, there was no significant difference in signal intensities of mmu-miR-323-3p in the brainstem and the cerebral cortex (3.65±0.71, P=0.088) in SAMP8 mice (Fig. 7D, Table II). In SAMR1 mice, there were no significant differences in the signal intensities of either miRNA among the brain regions. These values were 6.45±0.19 in the brainstem, 6.75±0.25 in the hippocampus (P=0.806) and 6.95±0.42 in the cortex (P=0.284) for mmu-miR-30e-3p (Fig. 7C, Table II) and 4.14±0.71 in the brainstem, 4.71±0.55 in the hippocampus (P=0.761) and 4.59±0.66 in the cortex (P=0.894) for mmu-miR-323-3p (Fig. 7D, Table II).

Table I. Statistical analysis of four SAMP8 specifically regulated miRNAs in the brainstem between SAMP8 and SAMR1 mice.

miRNA	Fold change (SAMP8/SAMR1)	P-value
Upregulated		
mmu-miR-491-5p	1.645	0.0413
mmu-miR-764-5p	2.044	0.0049
Downregulated		
mmu-miR-30e-3p	0.620	0.0098
mmu-miR-323-3p	0.342	0.0114

The fold change was calculated as the average signal intensity (non-log transformed). SAMP8, senescence-accelerated mouse prone 8; SAMR1, senescence-accelerated mouse resistant 1; mmu, *Mus musculus*; miRNA, microRNA.

The mean ΔCq ± standard deviation, based on RT-qPCR analysis, of mmu-miR-30e-3p in SAMP8 mice was 1.49±1.10, 1.18±0.79, 1.60±1.75 and that in SAMR1 mice was 1.13±0.73, 1.02±0.23 and 1.41±1.56 in the brainstem, hippocampus and cerebral cortex, respectively (Fig. 8C and Table III). Similarly, for mmu-miR-323-3p, the values in SAMP8 were 1.76±1.86, 1.13±0.59 and 1.32±1.05 and those in SAMR1 were 1.16±0.70, 1.03±0.28 and 1.66±2.22 in the brainstem, hippocampus and cerebral cortex, respectively (Fig. 8D and Table III). Overall, there were no significant differences in the miRNA expression levels, determined using RT-qPCR, among the brain regions of SAMP8 and SAMR1 mice.

miRNA target gene bioinformatics analysis. The target genes of differentially expressed miRNAs were predicted using three databases (miRDB, Targetscan and miRTarBase) and the overlapping genes in two or three databases were identified to enhance the reliability of the analysis. There were 5 target genes for mmu-miR-491-5p, 15 for mmu-miR-764-5p, 9 for mmu-miR-30e-3p and 7 for mmu-miR-323-3p. A Sankey diagram was used to examine whether there were any common target genes for each miRNA, but none were found (Fig. 9).

Discussion

Previous studies have reported that certain miRNAs are downregulated in the cerebral cortex and hippocampus of SAMP8 mice compared with SAMR1 mice, which indicates that these miRNAs may be involved in regulating genes associated with age-related brain changes (16). In the present study, two upregulated miRNAs (mmu-miR-491-5p and mmu-miR-764-5p) and two downregulated miRNAs (mmu-miR-323-3p and mmu-miR-30e-3p) were identified using 5-month-old SAMP8 mice, which displayed significant differential expression in the brainstem compared with the hippocampus and cerebral cortex. Age-related histopathological degeneration in the human brain occurs first in the brainstem and subsequently spreads to the hippocampus and cerebral cortex (8). Therefore, the observed changes in miRNA expression levels could trigger age-related brain degeneration. Herein, the cognitive deficits and brain pathological changes in the 5-month-old SAMP8 mice and the implications of the differentially expressed miRNAs are discussed.

In the Y-maze test, spontaneous alternation indicated short-term memory loss and spatial working memory impairment, which are classified as hippocampus-dependent memories (17). There were no significant differences in the alternation behavior rate between 5-month-old SAMP8 and SAMR1 mice and spatial working memory was preserved in SAMP8 mice. SAMP8 mice aged 6-8 months have been reported to demonstrate significant cognitive impairment compared with age-matched control SAMR1 mice (18,19). The data reported in the present study are consistent with these previous reports. The locomotive activity counts were significantly higher in SAMP8 mice compared with SAMR1 mice. One-month-old SAMP8 mice were reported to be more hyperactive than age-matched SAMR1 mice in a previous study (20). The results of the present study confirm that 5-month-old SAMP8 mice are hyperactive and are in a preliminary stage of spatial working memory impairment.

Spongiform degeneration and vacuoles were observed solely in the brainstem and astrocytes were found in the reticular formation of SAMP8 mice, whereas no pathological changes were reported in the hippocampus or cerebral cortex of SAMP8 mice or the brain of SAMR1 mice. The results of the present study were consistent with those of previous studies (11-13). In SAMP8 mice, spongiform degeneration in the brainstem reportedly begins at 1 month of age and reaches the maximum extent at 4-8 months of age (14). Moreover, vacuolization appears at 1 month of age in the brainstem reticular formation and the vacuoles increase in both size and number up to 8 months of age in SAMP8 mice (13). In humans, pathological changes in neurodegenerative diseases, such as AD and PD, occur in the brainstem during the early stages of disease and progress ascendingly to the other brain areas over time (9,21). In the present study, 5-month-old SAMP8 mice demonstrated age-related pathological changes exclusively in the brainstem, which suggested that the changes observed in 5-month-old SAMP8 mice correspond to the early stage of Braak staging in humans (8,21).

Although miRNA expression levels in each brain region have not been evaluated previously, increased expression of miR-491 has been reported in the whole brain of amyloid precursor protein (APP) and presenilin 1 double-transgenic mice at both 3 and 6 months of age (22). miR-491 serves an important role in various cancers, such as non-small cell lung cancer (23), osteosarcoma (24) and glioma (25), however only a single report describes its association with neurodegenerative diseases (22). In SAMP8 mice, the signal intensities of miR-491-5p were significantly different between the brainstem and other brain regions. This could indicate that changes in the levels of miR-491-5p expression precede changes in cognitive function. In the present study, miR-491-5p was upregulated in the brainstem of SAMP8 mice, wherein age-related degeneration occurs early.

Overexpression of miR-764 suppresses the expression of ninjurin 2 (NINJ2), an adhesion molecule expressed on neurons and glial cells that promotes the survival of human neurons and induces a significant decrease in neuronal

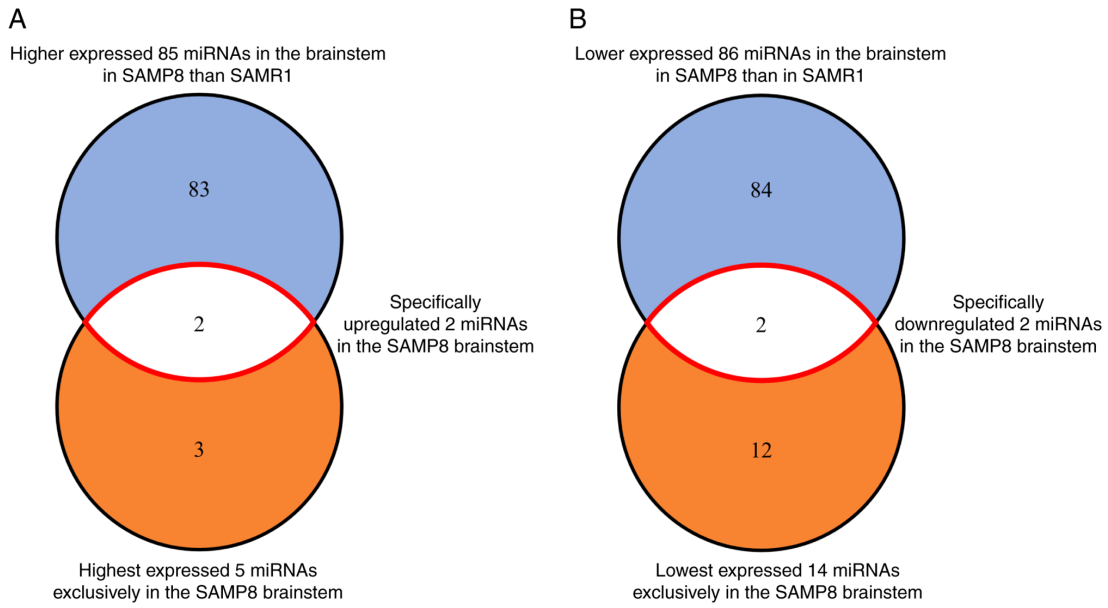

Figure 5. Venn diagrams of the SAMP8 brainstem specifically regulated miRNAs. (A) Two miRNAs were identified as specifically upregulated miRNAs in the SAMP8 brainstem from the Venn diagram in the set of two miRNAs with the highest expression exclusively in the SAMP8 brainstem and the set of 85 miRNAs with higher expression in the brainstem in SAMP8 than those in SAMR1. (B) Two miRNAs were identified as specifically downregulated miRNAs in the SAMP8 brainstem from the Venn diagram in the set of 14 miRNAs with the lowest expressed exclusively in the SAMP8 brainstem and the set of 86 miRNAs with lower expression in the brainstem in SAMP8 than in SAMR1. SAMP8, senescence-accelerated mouse prone 8; SAMR1, senescence-accelerated mouse resistant 1; miRNA, microRNA.

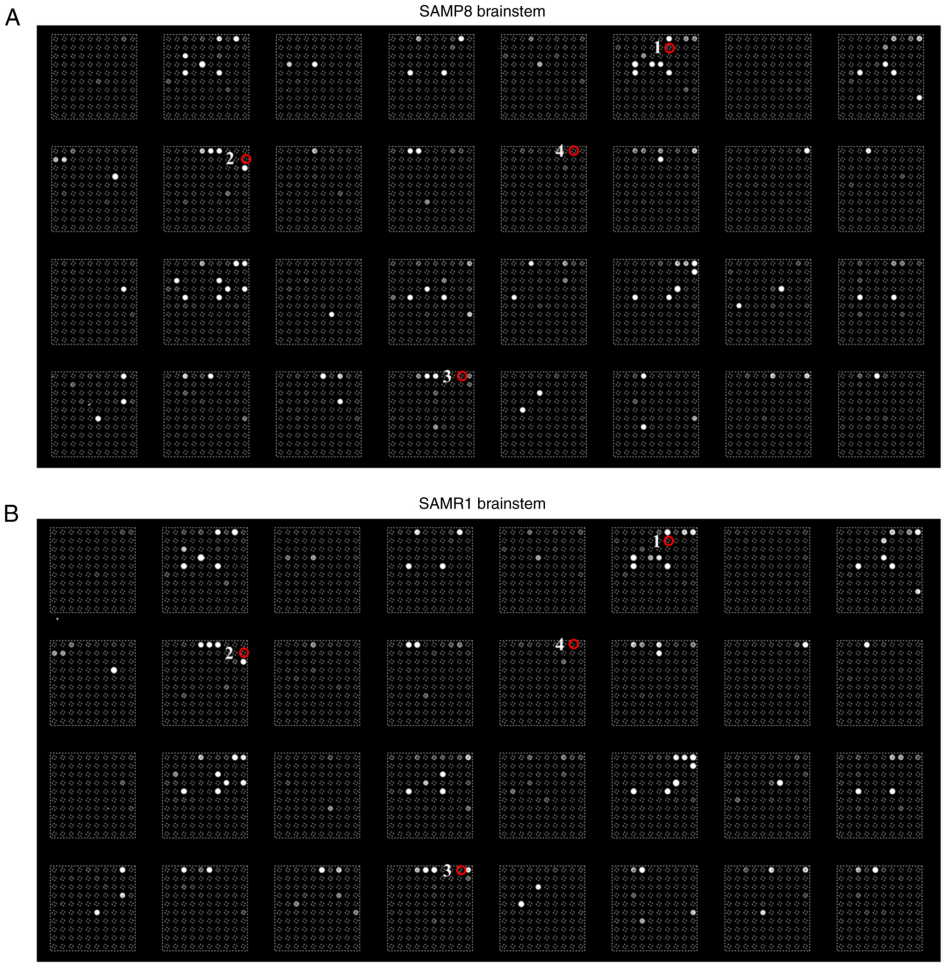

Figure 6. miRNA expression in the brainstems of (A) SAMP8 and (B) SAMR1 mice, analyzed using a miRNA chip. Spot numbers are presented as red circles. 1, miR-491-5p; 2, miR-764-5p; 3, miR-30e-3p; 4, miR-323-3p; SAMP8, senescence-accelerated mouse prone 8; SAMR1, senescence-accelerated mouse resistant 1; miRNA, microRNA.

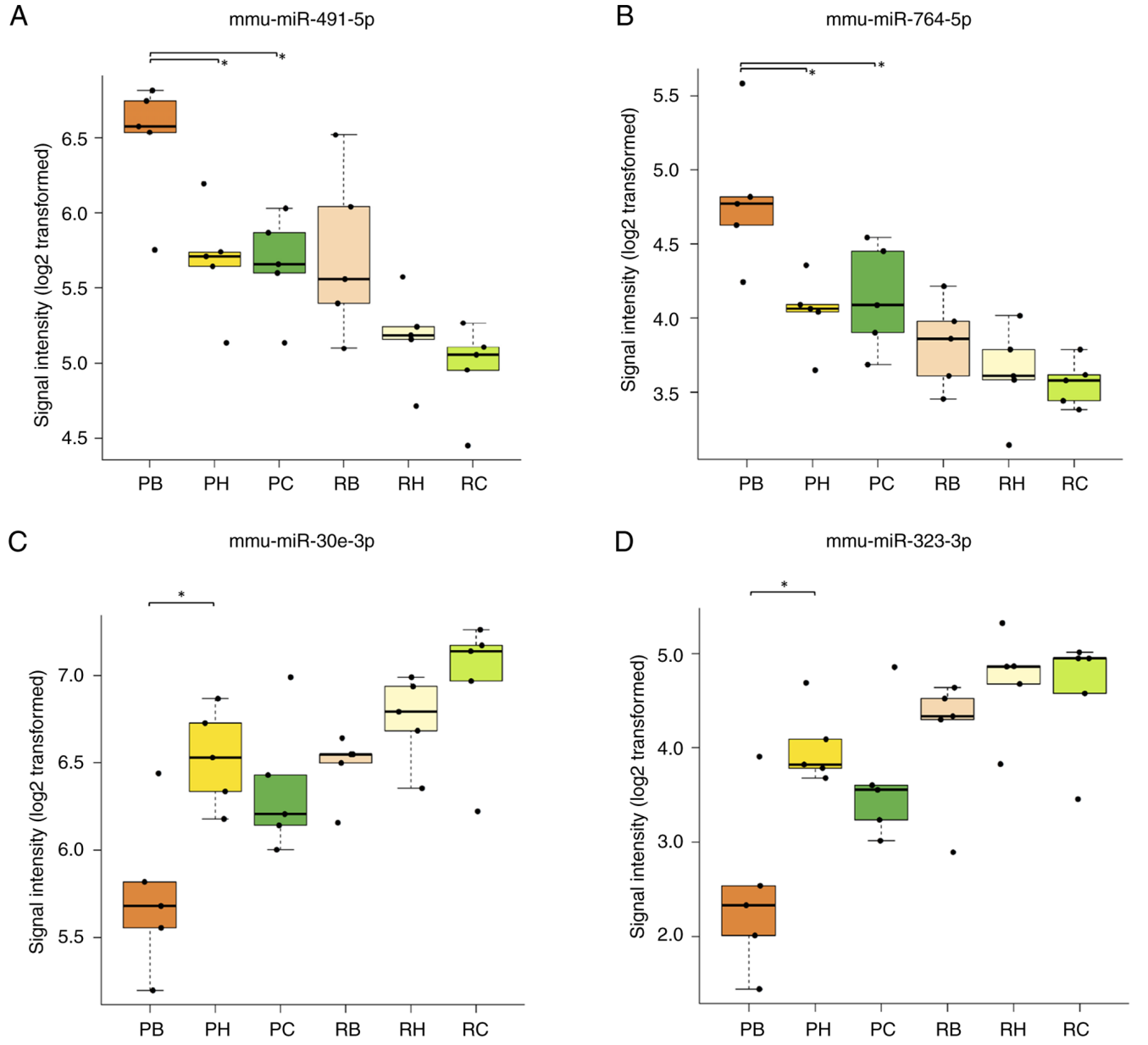

Figure 7. Signal intensities of (A) miR-491-5p, (B) miR-764-5p, (C) miR-30e-3p and (D) miR-323-3p in SAMP8 and SAMR1 mice. The results are shown as mean ± SD. *P<0.05. SAMP8 (P), senescence-accelerated mouse prone 8; SAMR1 (R), senescence-accelerated mouse resistant 1; B, brainstem; H, hippocampus; C, cerebral cortex; mmu, *Mus musculus*; miRNA, micro RNA.

survival and apoptosis (26). Thus, miR-764 acts as a promoter of neuronal growth by modulating NINJ2 expression (26,27). miR-764-5p was upregulated in the brainstems of SAMP8 mice, which indicated that neuronal apoptosis was induced in the brainstem and, consequently, age-related degeneration is likely to first occur in the brainstem.

Although miR-30e-3p and miR-323-3p were selected as specifically downregulated miRNAs by selection using the Venn diagram, post hoc tests of the signal values of each miRNA failed to detect significant differences between the brainstem and hippocampus of SAMP8. In the selection process using Venn diagrams, miRNAs that showed differences in signal intensities in the SAMP8 brainstem and hippocampus ($P<0.05$ and $FC<1.5^{-1}$) were included in the dataset. However, although Tukey's post-hoc test was performed on the signal intensities in all 6 groups of each brain region of SAMP8 and SAMR1, no significant differences were detected among the signal intensities of the brainstem and hippocampus in SAMP8. Instead, the signal intensity of specifically downregulated miRNAs tended to be the smallest in the brainstem compared with that in other brain regions of SAMP8 mice. More stringent selection criteria of specifically regulated miRNA candidates could make it difficult to detect miRNAs that may trigger early brain degeneration.

Analysis of the temporal lobe of the postmortem brains of patients with AD has previously demonstrated that miR-30e-3p activity is downregulated compared with that in the brains of patients without AD (28). In the present study, the expression of miR-30e-3p was specifically downregulated in the brainstem of SAMP8 mice. Moreover, target prediction indicated that miR-30e-3p downregulation may activate phosphatase and tensin homolog (PTEN) function, which may induce

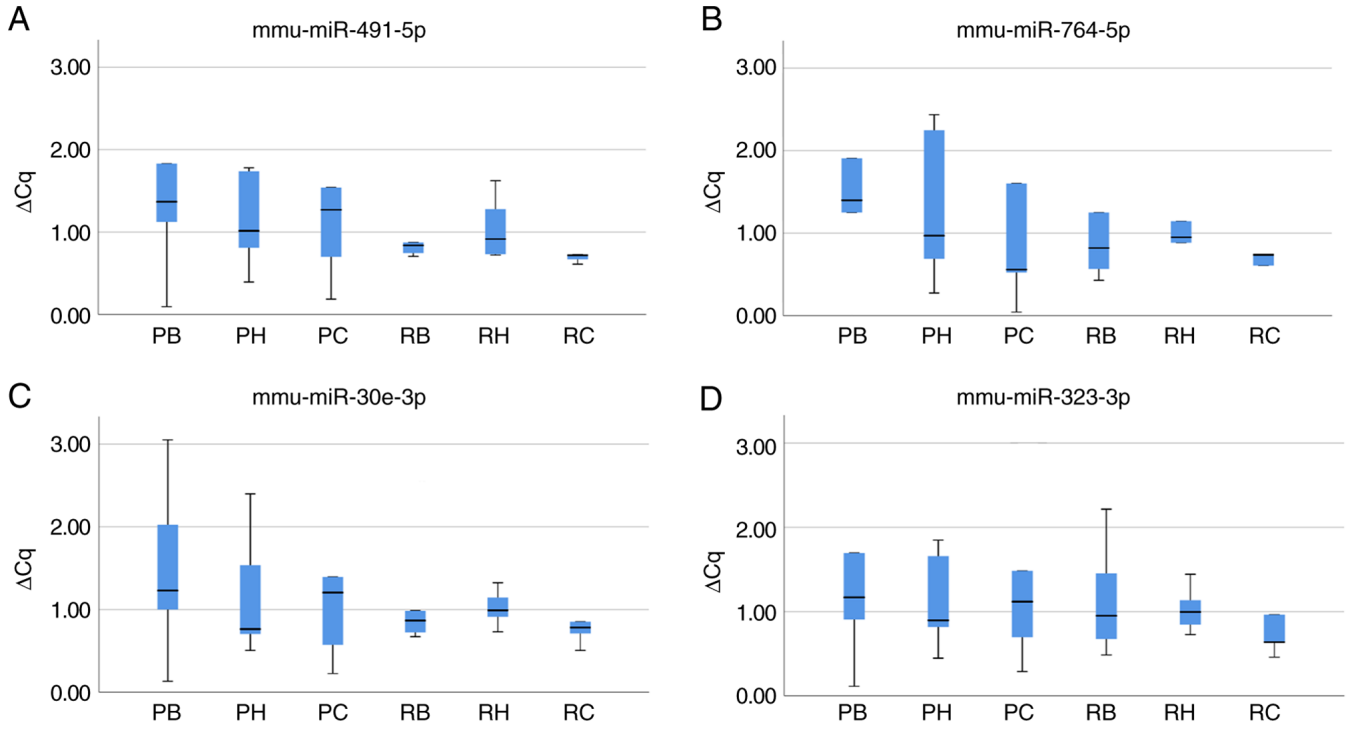

Figure 8. Expression levels based on reverse transcription-quantitative polymerase chain reaction analysis of (A) miR-491-5p, (B) miR-764-5p, (C) miR-30e-3p and (D) miR-323-3p in SAMP8 and SAMR1 mice. The results are shown as mean ± SD. SAMP8 (P), senescence-accelerated mouse prone 8; SAMR1 (R), senescence-accelerated mouse resistant 1; B, brainstem; H, hippocampus; C, cerebral cortex; mmu, *Mus musculus*; miRNA, micro RNA.

apoptosis in the central nervous system (29,30). Therefore, it could be inferred that apoptosis may be more likely occur in the brainstem.

miR-323-3p has been reported to reduce APP expression *in vitro* and under intracellular physiological conditions (31). The accumulation of APP leads to the overproduction, accumulation and deposition of amyloid-β, which ultimately leads to neuronal death (32). Moreover, miR-323-3p binds to transforming growth factor-β2 (TGF-β2) and suppresses the TGF-β2/c-Jun N-terminal kinase signaling pathway, thereby inhibiting cell apoptosis (33). In the present study, miR-323-3p was specifically downregulated in the brainstem of SAMP8 mice, which further indicates that apoptosis may occur in the brainstem and that APP expression is likely to occur in the brainstem, which leads to amyloidogenesis.

In the present study, the signal intensities of miR-30e-3p and miR-323-3p in the hippocampus of SAMP8 mice were generally higher than those in the cortex, which indicated that the signal intensity did not change according to Braak staging (8,21). The upregulation of miR-323-3p in the hippocampus compared with its expression in the cortex of SAMP8 mice may have been affected by the vulnerability of the hippocampus to various stressors (34). TGF-β2, regulated by miR-323-3p, suppresses the activation of neuronal-glial antigen 2 (NG2) glial cells as well as central nervous system progenitor cells and prevents inflammatory responses in the brain via TGF-β2-TGFBR2 signaling (35). NG2 glial cells are predicted to be involved in hippocampal vulnerability because NG2 glial cell ablation induces hippocampal neuronal cell death in rat models (36). Thus, the data presented in the present study suggests that neuroinflammation may be more likely to occur in the hippocampus and may, therefore, provide molecular evidence of the vulnerability of the hippocampus to age-related neurodegeneration.

The target genes of differentially expressed miRNAs were predicted using three databases (miRDB, Targetscan and miRTarBase) and the overlapping genes in two or more databases were identified to enhance the reliability of the analysis. PTEN, NINJ2 and TGF-β2 were not included as they were listed in individual databases but were not duplicated. Although the relationship between the identified miRNAs and the target genes (PTEN, NINJ2 and TGF-β2) involved in age-related brain changes had been previously reported (37-39), the present study provides evidence that such miRNAs may be related to target genes involved in age-related brain changes.

Specifically upregulated or downregulated miRNAs in the brainstem of SAMP8 mice were identified but no significant difference was noted in the expression levels of these miRNAs in the assessed brain regions, as determined using RT-qPCR. The progression of degeneration in 5-month-old SAMP8 mice was mild, therefore, it may be difficult to detect the difference in the expression levels of these miRNAs in the brain regions analyzed. Although it may be possible to detect significant differences in the expression levels of these miRNAs in older SAMP8 mice, identifying specific upregulated or downregulated miRNAs in the brainstem may be difficult owing to the progression of neurodegeneration. Furthermore, it is possible that there may be no noteworthy differences in the identified miRNAs using RT-qPCR. Nevertheless, the expression levels of these miRNAs were distinct across various brain regions, as demonstrated by the microarray analysis conducted in this study. These findings could serve as a foundational dataset for future SAM experimental studies.

Table II. Signal intensity of four SAMP8 brainstem specifically regulated miRNAs among the three brain regions of interest as investigated by custom microarray platform analysis.

mmu-miR	SAMP8 brainstem	SAMP8 hippocampus	SAMP8 cortex	SAMR1 brainstem	SAMR1 hippocampus	SAMR1 cortex	P-value for brain region comparison[a]	P-value for mouse type comparison[a]	P-value[b] (SAMP8 brainstem vs. SAMP8 hippocampus)	P-value[b] (SAMP8 brainstem vs. SAMP8 cortex)
491-5p	6.49±0.42	5.69±0.38	5.66±0.34	5.72±0.56	5.18±0.31	4.97±0.31	0.000291	0.000135	0.040	0.031
764-5p	4.81±0.49	4.04±0.25	4.13±0.36	3.82±0.30	3.63±0.32	3.56±0.16	0.000419	0.000131	0.013	0.036
30e-3p	5.74±0.45	6.53±0.28	6.35±0.39	6.45±0.19	6.75±0.25	6.95±0.42	0.00199	0.000368	0.015	0.866
323-3p	2.44±0.92	4.01±0.41	3.65±0.71	4.14±0.71	4.71±0.55	4.59±0.66	0.00436	0.000154	0.014	0.088

Signal intensity (log2) in the SAMP8 and SAMR1 groups are presented. The results are shown as mean ± SD. [a]Two-way ANOVA; [b]post-hoc test (Tukey's test); SAMR1, senescence-accelerated mouse resistant 1; SAMP8, senescence-accelerated mouse prone 8; mmu, *Mus musculus*; miRNA, microRNA.

Table III. Expression levels of four SAMP8 brainstem specifically regulated miRNAs determined using RT-qPCR in expression among the three brain regions of interest compared with SAMR1 mice.

mmu-miR	SAMP8 brainstem	SAMP8 hippocampus	SAMP8 cortex	SAMR1 brainstem	SAMR1 hippocampus	SAMR1 cortex	P-value for brain region comparison[a]	P-value for mouse type comparison[a]
491-5p	1.64±1.35	1.15±0.60	1.53±1.45	1.15±0.81	1.05±0.39	1.48±1.80	0.998	0.678
764-5p	2.10±2.23	1.32±0.96	10.51±21.98	1.42±1.49	1.19±0.83	2.17±3.49	0.496	0.472
30e-3p	1.49±1.10	1.18±0.79	1.60±1.75	1.13±0.73	1.02±0.23	1.41±1.56	0.975	0.860
323-3p	1.76±1.86	1.13±0.59	1.32±1.05	1.16±0.70	1.03±0.28	1.66±2.22	0.953	0.453

Results are shown as mean ± SD. [a]Two-way ANOVA; SAMR1, senescence-accelerated mouse resistant 1; SAMP8, senescence-accelerated mouse prone 8; mmu, *Mus musculus*; miRNA, microRNA.

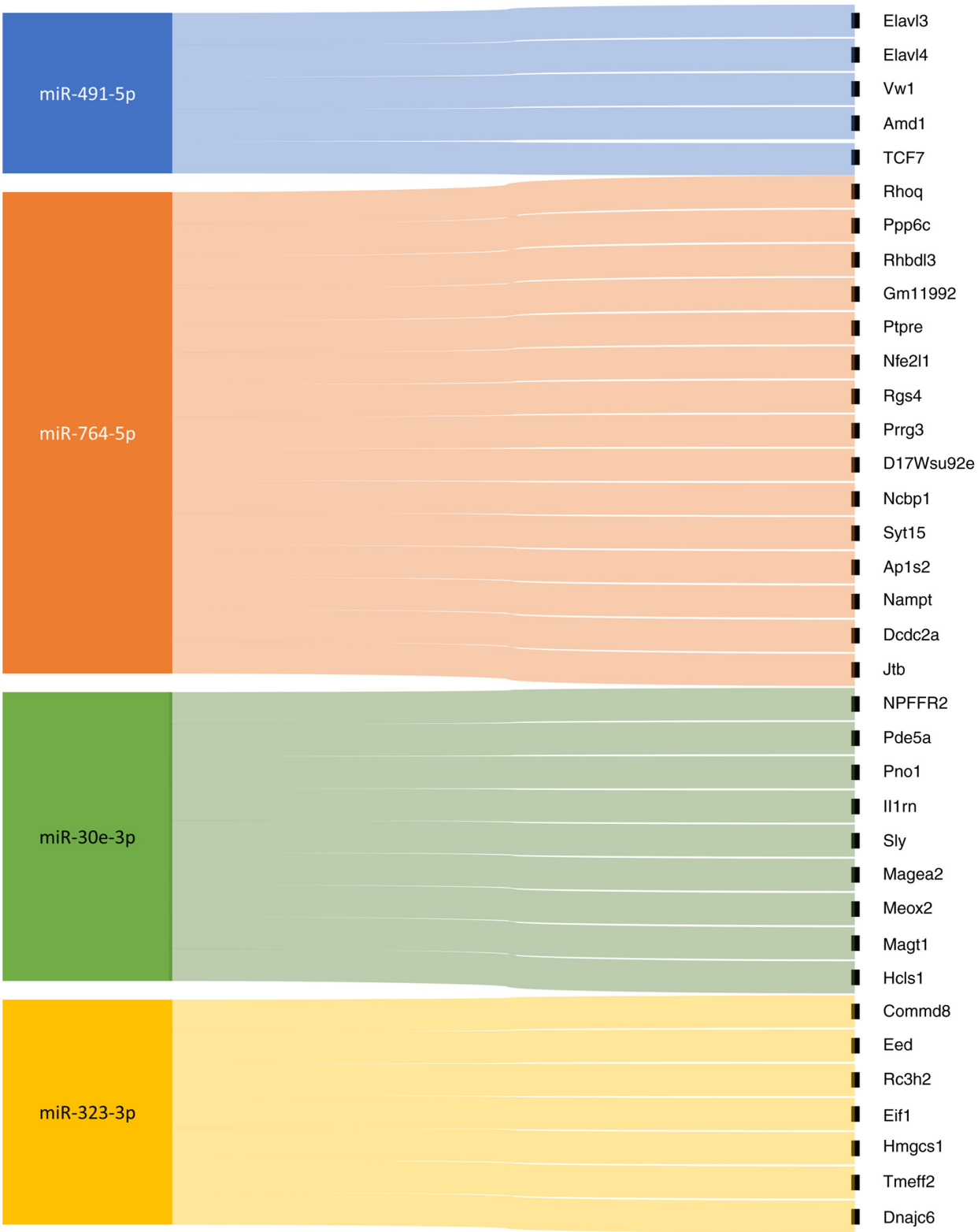

Figure 9. Target gene prediction of differentially expressed miRNAs. Sankey diagram of the four differentially expressed miRNAs and their respective target genes. miRNA, microRNA.

Specifically upregulated miRNAs (mmu-miR-491-5p and mmu-miR-764-5p) or downregulated miRNAs (mmu-miR-323-3p and mmu-miR-30e-3p) were identified in the brainstems of early postnatal SAMP8 mice. Furthermore, the mechanism by which miRNAs may regulate target proteins in the early stage of pathological degeneration in the brainstem to induce age-related neurodegenerative changes was investigated, thereby adding a new perspective to our understanding of neurodegenerative disease progression. Additionally, these miRNA changes may provide molecular evidence for the development of age-related pathological changes in the brain, as shown by Braak staging (8,21). Finally, the present study is the first to show that

four specific miRNAs (mmu-miR-491-5p, mmu-miR-764-5p, mmu-miR-323-3p and mmu-miR-30e-3p) were differentially expressed in the hippocampus and cortex in a stepwise manner. Furthermore, it was demonstrated that the expression levels of the same four miRNAs in the brainstem were specifically different compared with those in the hippocampus and cortex of SAMP8 mice, and the order of these miRNA expression levels tended to correspond with the progression order of age-related brain degeneration. Validation of these results in SAMP8 mice may reveal specific differences in miRNA expression levels in each brain region. To conclude, the present study has provided potential novel targets for future treatment options to delay the onset or progression of neurodegenerative diseases.

One potential limitation of the present study is the exclusive use of SAMP8 mice at 5 months old, when behavioral impairment is mild. It is plausible that utilizing SAMP8 mice of a more advanced aged could reveal distinct results. To achieve a comprehensive understanding of the miRNA changes associated with brain degeneration, further investigation is warranted in the future.

Acknowledgements

The authors would like to thank Mrs. Kayo Hirose, Mrs. Keiko Fujikawa, Mrs. Fuyuko Kokado and Mrs. Megumi Okamura (Kagawa University, Kagawa, Japan) for providing technical assistance with the experiments. The authors would also like to thank Mrs. Kayo Hosoi (Shikoku Cytopathological Laboratory, Kagawa, Japan) for preparing the pathological specimens.

Funding

This work was supported by JSPS KAKENHI (grant no. 22K17828).

Availability of data and materials

The datasets used/and or generated during the current study are available from the corresponding author upon reasonable request.

Authors' contributions

RK, TT, HI, TI, KD and TM conceptualized the study. RK, TT, WN and YH performed the experiments. RK, TT, HI, WN, YH and TI performed the formal analysis. RK, TT and HI developed the methodology. TI and TM were involved in project administration. KD and TM provided materials and funds for the study. HK, KD, OM and TM supervised the study. RK, TT, WN, YH, HK, KD, OM, TN and TI were involved in data validation. RK, TT and HI were involved in data visualization. RK and TT wrote the manuscript. TT, HI, HK, KD, OM, TN, TI and TM reviewed and edited the manuscript. All authors read and approved the final version of the manuscript. TT and TI confirm the authenticity of all the raw data.

Ethics approval and consent to participate

The present study was approved by the Animal Committee of the Kagawa University School of Medicine (approval number: 20626-2).

Patient consent for publication

Not applicable.

Competing interests

The authors declare that they have no competing interests.

References

1. Bartel DP: MicroRNAs: Target recognition and regulatory functions. Cell 136: 215-233, 2009.
2. Reddy PH, Williams J, Smith F, Bhatti JS, Kumar S, Vijayan M, Kandimalla R, Kuruva CS, Wang R, Manczak M, *et al*: MicroRNAs, aging, cellular senescence, and Alzheimer's disease. Prog Mol Biol Transl Sci 146: 127-171, 2017.
3. Salta E and De Strooper B: Non-coding RNAs with essential roles in neurodegenerative disorders. Lancet Neurol 11: 189-200, 2012.
4. Kume K, Iwama H, Deguchi K, Ikeda K, Takata T, Kokudo Y, Kamada M, Fujikawa K, Hirose K, Masugata H, *et al*: Serum microRNA expression profiling in patients with multiple system atrophy. Mol Med Rep 17: 852-860, 2018.
5. Nonaka W, Takata T, Iwama H, Komatsubara S, Kobara H, Kamada M, Deguchi K, Touge T, Miyamoto O, Nakamura T, *et al*: A cerebrospinal fluid microRNA analysis: Progressive supranuclear palsy. Mol Med Rep 25: 1-9, 2022.
6. Lees AJ, Hardy J and Revesz T: Parkinson's disease. Lancet 373: 2055-2066, 2009.
7. Braak H and Del Tredici K: The pathological process underlying Alzheimer's disease in individuals under thirty. Acta Neuropathol 121: 171-181, 2011.
8. Braak H and Del Tredici K: The preclinical phase of the pathological process underlying sporadic Alzheimer's disease. Brain 138: 2814-2833, 2015.
9. Braak H, Del Tredici K, Rüb U, de Vos RAI, Jansen Steur ENH and Braak E: Staging of brain pathology related to sporadic Parkinson's disease. Neurobiol Aging 24: 197-211, 2003.
10. Cheng XR, Zhou WX and Zhang YX: The behavioral, pathological and therapeutic features of the senescence-accelerated mouse prone 8 strain as an Alzheimer's disease animal model. Ageing Res Rev 13: 13-37, 2014.
11. Kawamata T, Akiguchi I, Yagi H, Irino M, Sugiyama H, Akiyama H, Shimada A, Takemura M, Ueno M, Kitabayashi T, *et al*: Neuropathological studies on strains of senescence-accelerated mice (SAM) with age-related deficits in learning and memory. Exp Gerontol 32: 161-169, 1997.
12. Kawamata T, Akiguchi I, Maeda K, Tanaka C, Higuchi K, Hosokawa M and Takeda T: Age-related changes in the brains of senescence-accelerated mice (SAM): Association with glial and endothelial reactions. Microsc Res Tech 43: 59-67, 1998.
13. Yagi H, Akiguchi I, Ohta A, Yagi N, Hosokawa M and Takeda T: Spontaneous and artificial lesions of magnocellular reticular formation of brainstem deteriorate avoidance learning in senescence-accelerated mouse SAM. Brain Res 791: 90-98, 1998.
14. Yagi H, Irino M, Matsushita T, Katoh S, Umezawa M, Tsuboyama T, Hosokawa M, Akiguchi I, Tokunaga R and Takeda T: Spontaneous spongy degeneration of the brain stem in SAM-P/8 mice, a newly developed memory-deficient strain. J Neuropathol Exp Neurol 48: 577-590, 1989.
15. Livak KJ and Schmittgen TD: Analysis of relative gene expression data using real-time quantitative PCR and the 2(-Delta Delta C(T)) method. Methods 25: 402-408, 2001.
16. Tan YX, Hong Y, Jiang S, Lu MN, Li S, Chein B, Zhang L, Hu T, Mao R, Mei R and Xiyang YB: MicroRNA-449a regulates the progression of brain aging by targeting SCN2B in SAMP8 mice. Int J Mol Med 45: 1091-1102, 2020.
17. Huang SM, Mouri A, Kokubo H, Nakajima R, Suemoto T, Higuchi M, Staufenbiel M, Noda Y, Yamaguchi H, Nabeshima T, *et al*: Neprilysin-sensitive synapse-associated amyloid-β peptide oligomers impair neuronal plasticity and cognitive function. J Biol Chem 281: 17941-17951, 2006.
18. del Valle J, Bayod S, Camins A, Beas-Zárate C, Velázquez-Zamora DA, González-Burgos I and Pallàs M: Dendritic spine abnormalities in hippocampal CA1 pyramidal neurons underlying memory deficits in the SAMP8 mouse model of Alzheimer's disease. J Alzheimers Dis 32: 233-240, 2012.

19. Miyamoto M: Characteristics of age-related behavioral changes in senescence-accelerated mouse SAMP8 and SAMP10. Exp Gerontol 32: 139-148, 1997.
20. Markowska AL, Spangler EL and Ingram DK: Behavioral assessment of the senescence-accelerated mouse (SAM P8 and R1). Physiol Behav 64: 15-26, 1998.
21. Braak H and Braak E: Neuropathological stageing of Alzheimer-related changes. Acta Neuropathol 82: 239-259, 1991.
22. Wang LL, Min L, Guo QD, Zhang JX, Jiang HL, Shao S, Xing JG, Yin LL, Liu JH, Liu R, *et al*: Profiling microRNA from brain by microarray in a transgenic mouse model of Alzheimer's disease. BioMed Res Int 2017: 8030369, 2017.
23. Gong F, Ren P, Zhang Y, Jiang J and Zhang H: MicroRNAs-491-5p suppresses cell proliferation and invasion by inhibiting IGF2BP1 in non-small cell lung cancer. Am J Transl Res 8: 485-495, 2016.
24. Wang SN, Luo S, Liu C, Piao Z, Gou W, Wang Y, Guan W, Li Q, Zou H, Yang ZZ, *et al*: miR-491 inhibits osteosarcoma lung metastasis and chemoresistance by targeting αB-crystallin. Mol Ther 25: 2140-2149, 2017.
25. Meng Y, Shang FR and Zhu YL: MiR-491 functions as a tumor suppressor through Wnt3a/β-catenin signaling in the development of glioma. Eur Rev Med Pharmacol Sci 23: 10899-10907, 2019.
26. Jing D, Yinzhu L, Jinjing P, Lishuang L and Guozhuan Z: Targeting ninjurin 2 by miR-764 regulates hydrogen peroxide (H2O2)-induced neuronal cell death. Biochem Biophys Res Commun 505: 1180-1188, 2018.
27. Araki T and Milbrandt J: Ninjurin2, a novel homophilic adhesion molecule, is expressed in mature sensory and enteric neurons and promotes neurite outgrowth. J Neurosci 20: 187-195, 2000.
28. Henriques AD, Machado-Silva W, Leite REP, Suemoto CK, Leite KRM, Srougi M, Pereira AC, Jacob-Filho W and Nóbrega OT; Brazilian Aging Brain Study Group: Genome-wide profiling and predicted significance of post-mortem brain microRNA in Alzheimer's disease. Mech Ageing Dev 191: 111352, 2020.
29. Chow LML and Baker SJ: PTEN function in normal and neoplastic growth. Cancer Lett 241: 184-196, 2006.
30. Shabanzadeh AP, D'Onofrio PM, Magharious M, Choi KAB, Monnier PP and Koeberle PD: Modifying PTEN recruitment promotes neuron survival, regeneration, and functional recovery after CNS injury. Cell Death Dis 10: 567, 2019.
31. Delay C, Calon F, Mathews P and Hébert SS: Alzheimer-specific variants in the 3'UTR of Amyloid precursor protein affect microRNA function. Mol Neurodegener 6: 70, 2011.
32. De Strooper B: Proteases and proteolysis in Alzheimer disease: A multifactorial view on the disease process. Physiol Rev 90: 465-494, 2010.
33. Shi CC, Pan LY, Zhao YQ, Li Q and Li JG: MicroRNA-323-3p inhibits oxidative stress and apoptosis after myocardial infarction by targeting TGF-β2/JNK pathway. Eur Rev Med Pharmacol Sci 24: 6961-6970, 2020.
34. Bartsch T and Wulff P: The hippocampus in aging and disease: From plasticity to vulnerability. Neuroscience 309: 1-16, 2015.
35. Zhang SZ, Wang QQ, Yang QQ, Gu HY, Yin YQ, Li YD, Hou JC, Chen R, Sun QQ, Sun YF, *et al*: NG2 glia regulate brain innate immunity via TGF-β2/TGFBR2 axis. BMC Med 17: 204, 2019.
36. Nakano M, Tamura Y, Yamato M, Kume S, Eguchi A, Takata K, Watanabe Y and Kataoka Y: NG2 glial cells regulate neuroimmunological responses to maintain neuronal function and survival. Sci Rep 7: 42041, 2017.
37. Knafo S, Sánchez-Puelles C, Palomer E, Delgado I, Draffin JE, Mingo J, Wahle T, Kaleka K, Mou L, Pereda-Perez I, *et al*: PTEN recruitment controls synaptic and cognitive function in Alzheimer's models. Nat Neurosci 19: 443-453, 2016.
38. Lin KP, Chen SY, Lai LC, Huang YL, Chen JH, Chen TF, Sun Y, Wen LL, Yip PK, Chu YM, *et al*: Genetic polymorphisms of a novel vascular susceptibility gene, Ninjurin2 (NINJ2), are associated with a decreased risk of Alzheimer's disease. PLoS One 6: e20573, 2011.
39. Peress NS and Perillo E: Differential expression of TGF-β 1, 2 and 3 isotypes in Alzheimer's disease: A comparative immunohistochemical study with cerebral infarction, aged human and mouse control brains. J Neuropathol Exp Neurol 54: 802-811, 1995.